Logarithmic decay of the orientational correlation function in supercooled liquids on the Ps to Ns time scale

Hu Cang, V. N. Novikov,[a] and M. D. Fayer
Department of Chemistry, Stanford University, Stanford, California 94305

(Received 16 September 2002; accepted 15 November 2002)

Dynamics of supercooled ortho-terphenyl, salol, benzophenone, 2-biphenylmethanol, and dibutylphthalate have been studied using optical heterodyne detected optical Kerr effect experiments over a broad range of time, <1 ps to tens of ns. On time scales longer than those influenced by intramolecular vibrational dynamics, ''intermediate'' power law decays with temperature independent exponents close to -1 have been observed from ~ 2 ps to 1–10 ns in all five samples. The intermediate power law decays occur over a wide range of temperatures from well above to somewhat below T_c, the mode-coupling theory (MCT) critical temperature. The intermediate power law corresponds to approximately a logarithmic decay of the polarizability–polarizability (orientational) correlation function. The amplitude of the intermediate power law increases with increasing temperature as $[(T-T_c)/T_c]^{1/2}$. The intermediate power law decay is followed by a second longer time scale power law, and the final portion of the decay is exponential. As a framework for discussion, the results are compared to the quantitative predictions of the MCT. The observations are in contrast to the standard MCT for the longer time portions of the decays. The observed intermediate power law decays may be consistent with MCT if the dynamics occur in the part of the MCT parameter space near a high order singularity (end point case). © *2003 American Institute of Physics.* [DOI: 10.1063/1.1536612]

I. INTRODUCTION

The relaxation behavior of supercooled liquids and the nature of the glass transition have been intensely investigated in recent years using a variety of experimental techniques,[1] but the physical nature of the dynamics of molecules in supercooled liquids are still poorly understood. In this paper, the results of optical heterodyne detected optical Kerr effect (OHD-OKE) experiments on the supercooled liquids, benzophenone (BZP), and 2-biphenylmethanol (BPM) are presented, and the previously obtained OHD-OKE experimental results on ortho-terphenyl (OTP),[2] salol,[3] and dibutylphthalate (DBP) (Ref. 4) are reanalyzed. The OHD-OKE experiment measures the time derivative of the polarizability–polarizability correlation function (orientational correlation function). The experiments were conducted over a broad range of times ($<$ps to tens of ns), and a wide range of temperatures. The temperatures spanned went from well above the crystalline melting point to $\sim T_c$, the critical temperature in mode coupling theory (MCT). The data are excellent over the full range of times and temperatures permitting detailed examination of the functional forms of the decays. On the shortest time scales, <100 fs to ~ 1 ps, intramolecular vibrations strongly affect the data with pronounced oscillatory features.[2,3] For times longer than the intramolecular vibrational damping times, ~ 2 ps, all five supercooled liquids exhibit temperature independent power law decays, t^{-p}, from ~ 2 ps to 1–10 ns. The power law exponents, $-p$, are close to -1 in all five liquids. The results indicate that this intermediate time portion of the correlation function decays as $\log t$ or close to it. The amplitude of intermediate power law increases with temperature as $(T-T_c)^{1/2}$.

The mathematical formalism of mode coupling theory provides quantitative predictions that can be used to discuss the results of experiments. Some features of the experiments presented below and many other experimental observations are reasonably well described by the two-step case of MCT at temperatures well above the true glass transition temperature, T_g.[5,6] In the MCT description, the time dependence of the density–density correlation function (and the orientational correlation function[7–9]) consists of a fast temperature independent decay (the critical decay or fast β-process) followed by a ''plateau,'' which, in turn, eventually decays to zero through complete structural relaxation. The early time portion of the complete structural relaxation gives rise to a power law decay, the von Schweidler power law, followed by an exponential or approximately exponential decay, the slow α process. As the temperature is lowered from high temperature, the relaxation time of the α process lengthens dramatically, and, according to ideal MCT, it diverges at T_c, at which all fluctuations are frozen. In the MCT formalism, this situation corresponds to the A_2 type singularity, or fold bifurcation of the MCT equations at critical values of the control parameters, for example, the temperature or the packing fraction. The A_2 singularity is thought to be relevant in most supercooled systems.[5,6] The analyses of the minimum of the susceptibility in dielectric relaxation, light scattering and neutron scattering experiments, and computer simula-

[a]On leave from Institute of Automation and Electrometry of the Russian Academy of Sciences, Novosibirsk, 630090.

tions seem to confirm this picture, although deviations usually occur at temperatures close to T_c.[10]

Recently, it was shown that in some special systems another MCT representation could describe the relaxation dynamics. The ''endpoint'' scenario, which corresponds to a higher MCT singularity A_n, $n \geqslant 3$, leads to an approximately logarithmic decay of the correlation function. Systems with interparticle potentials that can be represented by hard core repulsive and square well short range attractive parts are expected to exhibit the logarithmic time dependent decay of the correlation function. Both analytical estimates and computer simulations confirm that there is a significant time interval over which this type of system exhibits a $\log t$ dependence of the density correlation function.[11–15] Such behavior was observed experimentally by photon-correlation spectroscopy of colloids.[16] In the frequency domain, the contribution to the susceptibility has a $1/f$ noise like spectrum. If the explanation for the experimental data is found in MCT, as currently understood, only unique conditions for the trajectory of the system in the space of parameters of the mode coupling functional will give rise to the $\log t$ dependence; these should occur only in very special systems like colloids.

The experimental results presented below are discussed in the context of MCT and the possibility of higher order MCT singularities, which may describe the relaxation dynamics of supercooled liquids under more general circumstances than has been appreciated. A MCT higher order singularity gives rise to an approximately $\log t$ decay of the correlation function, which will produce an OHD-OKE power law signal decay with exponent ~ -1, with amplitude increasing with temperature as $(T-T_c)^{1/2}$, which is consistent with observation. However, low molecular weight supercooled liquids are not described by the particular nature of the interactions that can give rise to the higher order singularity responsible for the $\log t$ decay. A possible explanation for the apparent universal manifestation of a MCT higher-order singularity is discussed. However, it is not clear that the refined data presented here are in complete accord with MCT. They do not fit the commonly used form of MCT (A_2 singularity), and the suggestion of the general applicability of a higher order singularity will have to be born out by formal theoretical analysis.

II. EXPERIMENTAL PROCEDURES

The optical heterodyne detected optical Kerr effect (OHD-OKE) experiment, a nonresonant pump–probe technique,[17,18] measures the time derivative of the polarizability–polarizability correlation function (orientational correlation function).[19,20] The pump pulse induces an optical anisotropy. The induced optical anisotropy decays because of orientational relaxation. The decay is measured with a time delayed probe pulse. The Fourier transform of the OHD-OKE signal is directly related to data obtained from depolarized light scattering,[21,22] but the time domain OHD-OKE experiment can provide better signal to noise ratios over a broader range of times for experiments conducted on very fast to moderate time scales.

When sufficiently short excitation pulses are used ($\leqslant$70 fs), the correspondingly large bandwidth excites an orientationally anisotropic distribution of librations via stimulated Raman scattering. The damping of the optically excited librations leaves behind a residual molecular orientational alignment. When the excitation pulses are longer, the corresponding bandwidth is insufficiently broad to drive librational motions by stimulated Raman scattering. Rather, the $\boldsymbol{E}$ field associated with longer pulses exerts a torque on molecules with a polarizability anisotropy, which results in a molecular orientational anisotropy along the direction of the applied $\boldsymbol{E}$ field. In either case, the resulting orientational anisotropy gives rise to an optical birefringence in the sample, which is monitored by the probe pulse. A pulsed probe beam, in conjunction with two delay lines (0–600 ps and 0–30 ns), was used for monitoring decays up to 30 ns. For longer decay times, following pulsed excitation, a CW probe beam and a fast digitizer were employed to measure the decay.

A homebuilt Ti:sapphire oscillator and regenerative amplifier provided the pulses. The amplifier was pumped by a Q-switched, intracavity double Nd:YAG laser. The system produced 400 μJ pulses (prior to compression) at a repetition rate of 5 kHz, centered at 800 nm. An adjustable grating compressor permitted pulse durations of $<$70 fs to 2 ps (FWHM) to be obtained. The longer pulses are achieved by incomplete compression. In addition, bypassing the grating compressor entirely yields pulses of $\sim$100 ps FWHM. The partially compressed and uncompressed pulses are chirped. The use of chirped pulses does not interfere with the production or detection of the optical Kerr effect because it is a nonresonant experiment. The shortest pulses were used to resolve the fastest time-scale data. Better signal to noise ratios were obtained at long times by using longer pulses with greater average power. The CW probe was obtained from a commercial diode laser, centered at 635 nm, with an output power of 15 mW.

In an optical Kerr experiment, the sample is placed between crossed polarizers, and it is pumped with a polarization that is at 45° to the probe polarization. Optical heterodyne detection[17,18] employs a slightly rotated quarter wave plate in the probe beam (pulsed or CW) following the first polarizer, resulting in improved signal to noise ratios and a linear signal in the third-order dielectric susceptibility. Data were collected over 4 distinct time ranges; 0–20 ps using 70 fs pulses and a 0.1 μm stepper motor delay line; 3–600 ps using 1 ps pulses and a 0.1 μm stepper motor delay line; 0.1–30 ns using 100 ps pulses and a 30 ns delay line; and 10 to several hundred ns using 100 ps pump pulses, a CW probe, and a fast digitizer. The significant overlap of each time range with the next longer range permitted the data sets to be merged by multiplication of the data amplitude until decays were coincident in the overlap region. Care was taken to insure data overlap between differing time scales was excellent.

Sample cuvettes (1 cm optical length) were cleaned on a distillation apparatus to remove dust and other contaminates. BZP and BPM were obtained from Aldrich and were purified by fractional vacuum distillation and sealed in the optical cuvettes while still attached to distillation apparatus. The experimental results for the other three liquids (OTP, salol, and DBP) have been reported previously;[2–4] the results for these

samples will be reinterpreted here. Temperature control was obtained using a constant flow cryostat, with temperature stability of ± 0.1 K.

III. THEORETICAL BACKGROUND

MCT provides quantitative predictions for the dynamics of supercooled liquids, and it has been used to interpret many experiments. Therefore, it will be used as a reference point for comparison to the experimental data, and it is briefly outlined here. MCT states that the glass transition is a kinetic phenomenon caused by a nonlinear feedback mechanism. The theory starts from the generalized Langevin equation,[5,6]

$$\partial_t^2 \phi_q(t) + \Omega_q^2 \phi_q(t) + \int_0^t d\tau M_q(t-\tau)\partial_\tau \phi_q(\tau) = 0, \qquad (1)$$

where the $\phi_q(t)$ are a set of density correlation functions or correlation functions of other physical variables (orientation) that are coupled to the density, and the Ω_q are characteristic frequencies. MCT expands the kernel $M_q(t)$ into two parts, $M_q(t) = M_q^{\mathrm{reg}}(t) + \Omega_q^2 m_q(t)$, the regular part $M_q^{\mathrm{reg}}(t)$ and the mode coupling part $m_q(t)$. The mode coupling part $m_q(t)$ is a functional of the correlation functions $\phi_q(t)$: $m_q(t) = F_q[V,\{\phi\}]$ that brings in the nonlinear feedback mechanism. The functional depends smoothly on the control parameters V, for example, temperature or density. Expanding the functional using a Taylor series, for the one component model, for example, $m = \Sigma_{k=0}^{N} \lambda_k \phi^k$, one gets a set of parameters λ_k that form an N dimensional parameter space. N, in the general case, can be infinity; however, in schematic models only a few terms are taken into account. The parameter space splits into regions of glassy states and liquid states. The hypersurface, S, that separates supercooled liquid and glassy states corresponds to the glass transition in ideal MCT. Different types of singularities can be classified as A_l, $l = 2, 3, \ldots$. Near the simplest singularity, A_2, MCT predicts a two-step relaxation process consisting of a fast β process followed by a slow α process.

The long time tail of the β process, to first order, is characterized by a power law decay,

$$\phi_q(t) = f_q^c + |\sigma|^{1/2} h_q \left(\frac{t}{t_\sigma}\right)^{-a}, \qquad (2)$$

where σ is the separation parameter, f_q^c is the Debye–Waller factor, which determines the plateau level, $t_\sigma = t_0 |\sigma|^{-1/2a}$ is a rescaling time. The microscopic time t_0 is a constant, and the exponent $a < 0.5$. The separation parameter $\sigma = (T - T_c)/T_c$. For temperatures above the MCT critical temperature T_c, the decay away from the plateau is another power law called the von Schweidler power law,

$$\phi_q(t) = f_q^c - |\sigma|^{1/2} B \left(\frac{t}{t_\sigma}\right)^{b}, \quad B > 0. \qquad (3)$$

The von Schweidler power law decay is the onset of the α-relaxation, which is usually described by an exponential or stretched exponential function having decay constant, τ_α. The two exponents a and b are related through the exponent parameter λ via

$$\lambda = \Gamma^2(1-a)/\Gamma(1-2a) = \Gamma^2(1+b)/\Gamma(1+2b). \qquad (4)$$

In frequency domain experiments, in the two-step scheme above T_c there is a minimum between two power laws in the dynamic susceptibility spectra.

The power laws given in Eqs. (2) and (3) are the leading terms of the power law expansions[23,24] of the correlation function describing the fast β process (critical decay),[25] which is the full solution to the kinetic equations arising in MCT. These equations are solved numerically. The power law expansions approximate the numerical solutions. More extended results of ideal MCT, including higher order terms,[24] have been used to describe experimental data over larger ranges of time or frequency.[2–4,26–29] Using the higher order terms, the behavior between the limiting power laws given in Eqs. (2) and (3) can be calculated with 1% accuracy.[24] The extended forms of Eqs. (2) and (3) are, for times $t_0 < t \leq t_\sigma$,

$$\phi_q(t) = f_q^c + h_q |\sigma|^{1/2} [(t/t_\sigma)^{-a} - A_1 (t/t_\sigma)^{a} + A_2 (t/t_\sigma)^{3a} - A_3 (t/t_\sigma)^{5a} + \cdots], \qquad (5)$$

and for $t_\sigma < t \leq \tau_\alpha$,

$$\phi_q(t) = f_q^c + h_q |\sigma|^{1/2} [-B(t/t_\sigma)^{b} + (B_1/B)(t/t_\sigma)^{-b} + \cdots]. \qquad (6)$$

Taking the higher order terms in the expansion of the correlation function into account, theoretical predictions can be compared to experimental data over a wide time window. The combined Eqs. (5) and (6) do not decay as $\log t$, and the time derivative of the combined Eqs. (5) and (6) does not describe an extended ''intermediate'' time scale power law. Therefore, the standard MCT description of dynamics obtained for the A_2 singularity cannot explain an OHD-OKE experimental observation of an intermediate power law.

MCT predicts that near higher order singularity, the structural relaxation process is governed by a logarithmic decay. The leading order contribution is[30,31]

$$\phi_q = f_q^c - B_1 h_q \log(t), \quad B_1 = \sqrt{6\sigma}. \qquad (7)$$

It has also been shown that this logarithmic decay can crossover to the von Schweidler power law decay at longer times.[30]

The OHD-OKE experiment measures the time derivative of the polarizability–polarizability correlation function,[32] which is equivalent to measuring the time derivative of the orientational correlation function that can be described by MCT.[7–9] Thus, in the time regime of the fast relaxation, to first order the OHD-OKE signal, $S_f(t)$, is proportional to

$$S_f \propto \frac{d\phi_q}{dt} = -a h_q (t/t_0)^{-a-1}, \qquad (8)$$

and in the von Schweidler regime to

$$S_{\mathrm{vS}} \propto \frac{d\phi_q}{dt} = -bB|\sigma|^{(a+b)/2a}(t/t_0)^{b-1}. \qquad (9)$$

The logarithmic term, if any, gives a contribution

$$S_{\log} \propto \frac{d\phi_q}{dt} = -B_1 h_q t^{-1}. \qquad (10)$$

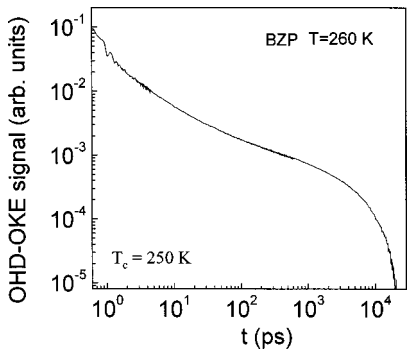

FIG. 1. OHD-OKE data for the supercooled liquid benzophenone at 260 K. At the shortest times, $t<2$ ps, oscillations originating from intramolecular vibrations strongly influence the signal. (The oscillations have an odd appearance because they are displayed on a log plot.) The longest time scale portion of the data ($t>\sim 1$ ns) is the exponential α-relaxation, which is immediately preceded by the von Schweidler power law. As discussed in detail below, from ~ 2 ps to the von Schweidler decay, an "intermediate" power law makes a major contribution to the signal.

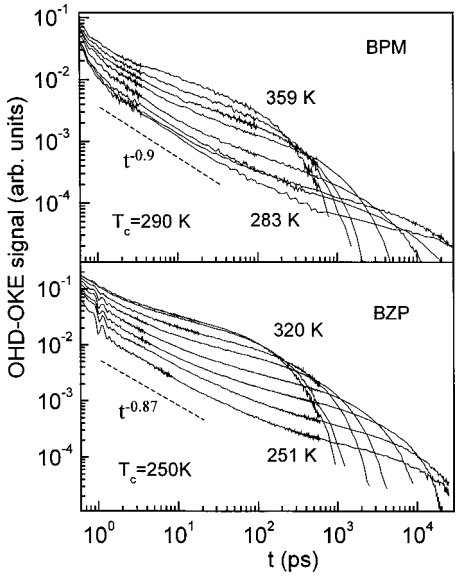

FIG. 2. The OHD-OKE signal in BPM and BZP is plotted vs time on the log plot for various temperatures. The temperature of each curve is, from the bottom, BPM: 283, 287, 291, 295, 299, 311, 323, 331, 343, 351, and 359 K, BZP: 251, 254, 260, 269, 281, 290, 302, 311, and 320 K. The dashed lines are aides to the eye showing the slopes of the intermediate power laws. The intermediate power laws are displayed more prominently in Figs. 5 and 6.

IV. RESULTS AND DISCUSSION

Figure 1 shows a typical data set taken on BZP at 260 K. The data are displayed on a log plot because of the large ranges of amplitude and time spanned, that is, over 4 decades of amplitude and almost 5 decades of time, from 600 fs to 20 ns. Although the decay functions change with temperature and from sample to sample, some common features are clear and can be seen in Fig. 1. The initial decay (<300 fs, not shown) is a combination of electronic and nuclear contributions.[33,34] Because of the short pulses (<70 fs) used for the earliest portion of the data, the electronic part of the OHD-OKE signal does not contribute to the signal for $t>300$ fs. In previous measurements at short times,[3] polarization selective TG-OKE experiments,[20] which eliminate the electronic contribution to the signal, were used to measure the decays for $t<300$ fs. These measurements confirm that the OHD-OKE data are free of an electronic contribution for $t>300$ fs. Low frequency internal molecular vibrations excited by stimulated Raman scattering are seen as oscillations in the signal up to ~ 2 ps. Because of the log time axis, the oscillations appear more closely spaced as the time gets longer. The structure of the signal in this time regime is complex. In addition to the oscillations, the signal decays over this period. Because of the oscillations, the data analysis presented below will consider $t\gtrsim 2$ ps.

Once the oscillations are damped, the subsequent decay of the signal can be subdivided into different sections. On the longest time scale ($\gtrsim 1$ ns), the α-relaxation occurs. The decay is well modeled as exponential with decay times, τ_α, increasing with decreasing temperature. On the log plot shown in Fig. 1, the exponential decay appears as the steep descent following the more gradual decay at shorter times. Just prior to the onset of the exponential α-relaxation is the von Schweidler power law [Eqs. (9) and (3)], characterized by the exponent, b. At the shortest times, partially masked by the oscillations, is another power law, the critical decay or the fast β process [Eqs. (8) and (2)], characterized by the exponent, a. MCT states that the slope of the OHD-OKE data is $-1-a$ with $a>0$; the slope becomes steeper at shorter times.

Between the fast β process and the von Schweidler power law is a region that has generally been described in terms of Eqs. (5) and (6). All of the data sets have the same general form, but major features (power law exponents, final exponential decays) occur on different time scales depending on the temperature and sample. However, instead of the OHD-OKE curve between the fast β process and the von Schweidler power law having a form that is obtained from the time derivative of Eqs. (5) and (6), the detailed analysis given below demonstrates that the data in this time range in all five liquids is an "intermediate" power law with temperature independent exponent. Such an intermediate power law is more consistent with Eq. (10) [the time derivative of Eq. (7)].[35] Initial reports of the intermediate power law incorrectly described it as having a temperature dependent exponent.[2–4]

Figure 2 displays temperature dependent data for the liquids BPM [$T_g\approx 239$ K (Ref. 36)] and BZP [$T_g\approx 212$ K (Ref. 37)]. The data are shown for various temperatures from $\sim T_c$ to well above T_c. All curves are normalized at $t=0$. The determination of T_c will be discussed below. Analogous data for the other three liquids, salol, OTP, and DBP, have been reported previously[2–4] and are reanalyzed here. Also shown in Fig. 2 are dashed lines that serve as an aid to the eye. The lines are drawn with the slopes of the intermediate power laws determined using the procedure discussed below. More detailed views of the power law portions of the decays are also presented below.

The data shown in Fig. 2 and the analogous data for salol, OTP, and DBP were fit for $t\gtrsim 2$ ps using a mode coupling like asymptotic expression, but including a term that

corresponds to the intermediate power law decay. The fitting function, $F(t)$, has the form,

$$F(t)=[pt^{-1+c}+dt^{b-1}]\exp(-t/\tau_a). \tag{11}$$

The first term with $c\ll 1$ corresponds to the intermediate power law; the second term is von Schweidler power law; the exponential function describes the final α-relaxation decay. The product of the von Schweidler power law and the exponential have been previously shown to describe the longer time portion of the OHD-OKE data for several supercooled liquids extremely well.[2–4] Frequently, the long time portion of the correlation function is described as a stretched exponential. The time derivative yields a product of a power law times a stretched exponential. Using a stretched exponential adds another power law and more parameters in the fit. We found that employing the time derivative of a stretched exponential did not improve the fit. Furthermore, the form used to fit the long time scale α-relaxation, so long as it is a good fit, does not influence the fit of the intermediate power law at much shorter times.

The OHD-OKE experiment is related to the susceptibility spectrum by the Fourier transform as[32]

$$S(t)=2F^{-1}\{\mathrm{Im}[D(\omega)]\},$$

where $S(t)$ is the OHD-OKE signal; $\mathrm{Im}[D(\omega)]$ is directly comparable with dynamic light scattering experiments. The t^{-1+c} decay in time domain corresponds to the near constant loss (NCL) spectrum in the susceptibility and $1/f$ noise in the power spectral density. Consequently, NCL is exactly the equivalent of the intermediate power law in frequency domain. The term $t^{b-1}\exp(-t/\tau_\alpha)$ in Eq. (11) in the frequency domain corresponds to imaginary part of the Cole–Davidson function $1/(1-i\omega t)^b$,[38] which is often used to describe the α-relaxation peak.

To obtain the best fit, the two power law exponents and the exponential time constant are determined by globally fitting all temperature curves for $t\geqslant 2$ ps. The exponential decay constant is essentially independent of the other parameters and easily determined. When each curve was fit individually, the results were basically the same. In particular, the intermediate power law exponents have the same values within experimental error, and they are temperature independent. The global fit is useful at the higher temperatures at which the von Schweidler power law spans only a short range, and its exponent is difficult to determine. In Fig. 3 the fits for some selected temperatures are shown for BZP and BPM. The data for the other three liquids are fit equally well. As one can see from Fig. 3, Eq. (11) does a very good job in fitting the decay curves at various temperatures from 2 ps to the end of the data (many ns). There is no systematic deviation between the data and the fits as T_c is approached or for temperatures below T_c, which indicates that the form of the curves is the same above and below T_c. The power law exponents and their amplitudes are very robust in these fits.

The analysis of the fitting parameters for the α-relaxation and the von Schweidler term were performed within the standard MCT approach. According to MCT, the α-relaxation time scales with temperature as

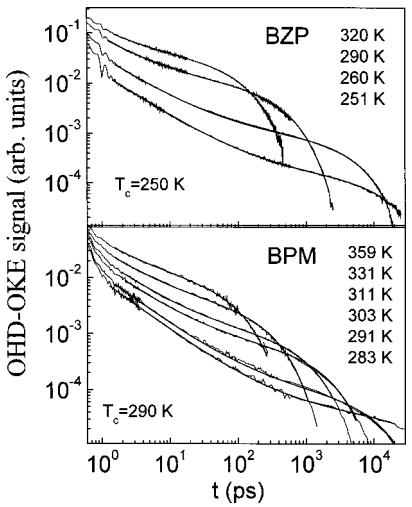

FIG. 3. BZP and BPM data and fits to Eq. (11) for some representative temperatures from 2 ps to the ends of the data. Equation (11) fits the data well over the full ranges of time and temperature.

$$\tau_\alpha^{-1/\gamma}\propto(T-T_c), \tag{12}$$

where $\gamma=(a+b)/2ab$. MCT also predicts[6] that the amplitude, d, of von Schweidler term scales with temperature above T_c as

$$d^{1/\delta}\propto(T-T_c), \tag{13}$$

where $\delta=(a+b)/2a$. The exponent a of the critical decay was obtained from Eq. (4) using the von Schweidler exponent b found from the fits. The respective rectification plots for BZP and BPM are presented in Fig. 4. Within the accu-

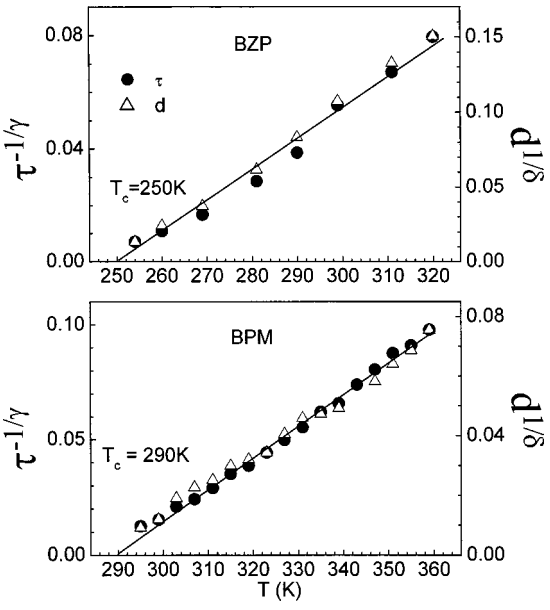

FIG. 4. The rectification diagrams for BZP and BPM. Left axis: the α-relaxation time τ_α is plotted as $\tau_\alpha^{-1/\gamma}$ [$\gamma=(a+b)/2ab$] vs temperature (circles). Right axis: the amplitude of the von Schweidler power law d is plotted as $d^{1/\delta}$ ($\delta=(a+b)/2a$) vs temperature (triangles). b is the von Schweidler power law exponent, and the relationship between a and b is given in Eq. (4). Within experimental error, both MCT scaling laws [Eqs. (12) and (13)] are obeyed and yield the same MCT critical temperature, $T_c=250$ K for BZP and 290 K for BPM.

TABLE I. The values of the exponents and critical temperatures.

	b	c	γ	δ	T_c
BZP	0.85±0.03	0.13±0.03	1.92	1.63	250±4
BPM	0.8±0.03	0.1±0.03	2.01	1.61	290±4
Salol	0.84±0.03	0±0.03	1.94	1.64	260±4
OTP	0.73±0.03	0.15±0.03	2.11	1.54	290±4
DBP	0.85±0.03	0.21±0.03	1.93	1.64	234±4

racy of the fits, both scaling laws, Eqs. (12) and (13), are confirmed, and for each liquid the two scaling laws yield the same critical temperature T_c. T_c was determined for the other three liquids in an analogous manner. Thus, the long time behavior of the relaxation is in agreement with the predictions of standard MCT. The values of T_c, b, γ, and δ are given in Table I.

Figure 5 displays log plots of the intermediate power law portions of the data for the five liquids with the contributions from the von Schweidler term and the α-relaxation removed. The data are straight lines over 3–4 decades of time. For each liquid at all temperatures, temperature independent intermediate time scale power law decays are seen. Figure 5 clearly displays the nature of the intermediate power law portion of the decays. The intermediate power law exponent in the OHD-OKE experiment is $-1+c$ [see Eq. (11)]. The values of c for each liquid are given in Table I. The intermediate power law exponents are temperature independent. This is demonstrated for BPM in Fig. 6. Within experimental error, the slopes of the lines are independent of temperature. This is true of the other liquids as well. In the initial observations of the intermediate power law,[2,3] it was reported that the power law exponents were temperature dependent. In the analysis employed initially, the contributions from the α-relaxation and the von Schweidler power law were not removed. The α-relaxation decay constant, τ_α, is highly temperature dependent, and the amplitude of the von Schweidler power law is also temperature dependent. Although the intermediate power law dominates the shorter time portion of the decay, the extent to which the temperature dependence of the longer time portions of the decay could influence the apparent slope of the intermediate power law at the higher temperatures was not appreciated. The previously reported intermediate power law exponents were approximately correct only at the lowest temperatures where the separation of time scales was very large.

The temperature dependence of the amplitude p of the intermediate power law term is shown in Fig. 7 in terms of the reduced temperature $(T-T_c)/T_c$ for 4 of the 5 liquids. (The normalization data necessary to obtain the temperature dependence of p was not taken for DBP.) The plot shows p^2 as a function of $(T-T_c)/T_c$. The line through the data is a fit to the points. The inset shows the points plotted as p versus $(T-T_c)/T_c$. The solid line is a fit with $p \propto [(T-T_c)/T_c]^{1/2}$. Figure 7 clearly demonstrates that the intensity of the intermediate power law is a square root function of $(T-T_c)/T_c$ in accordance with Eqs. (10) and (7). Therefore, the orientational correlation function decays with time and temperature dependencies that are consistent with the MCT endpoint case, that is, a high order ($n \geqslant 3$) singularity.

At high temperatures, the experimental curves can be fit reasonably well by the standard MCT two-step description of supercooled liquid dynamics (A_2 singularity) because the "slow" structural relaxation (α-relaxation) becomes so rapid that the intermediate power law region occurs over only a short interval. However, at lower temperatures, as T_c is approached, the time interval over which the intermediate power law dominates becomes so large (2 or more decades) that the experimental curves cannot be fit well with standard

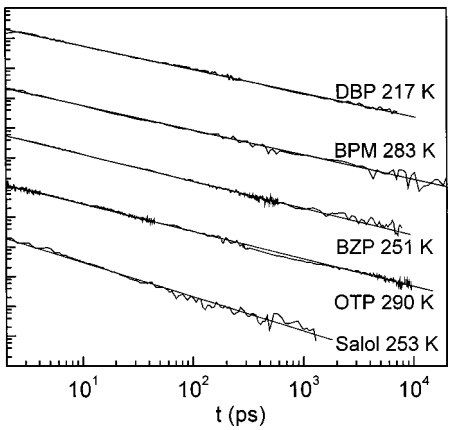

FIG. 5. Log plots of the intermediate power law portions of the data for the five liquids, DBP, BPM, BZP, OTP, and Salol at temperatures near T_c with the contributions from the von Schweidler term and the α-relaxation removed. The data are straight lines (power laws) over 3–4 decades of time, from 2 ps to ~1 to ~10 ns. The values of the power law exponents are $-1+c$. The c values are given in Table I. The curves have been displaced along the vertical axis for clarity of presentation.

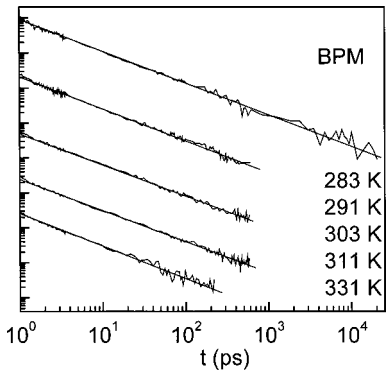

FIG. 6. Log plots of the intermediate power law portions of the BPM data for the five temperatures with the contributions from the von Schweidler term and the α-relaxation removed. The data demonstrate that the exponent of the intermediate power law is temperature independent. The curves have been displaced along the vertical axis for clarity of presentation.

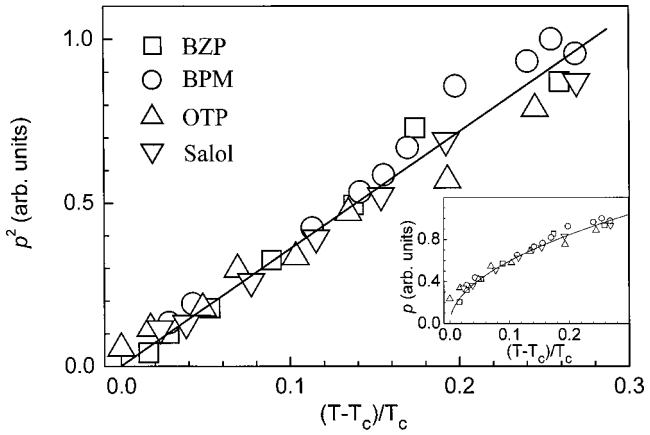

FIG. 7. The amplitudes p of the intermediate power laws of four liquids are plotted as p^2 vs $(T-T_c)/T_c$. The vertical scales are normalized so all plots overlap. The points fall on a line. Inset: p plotted vs $(T-T_c)/T_c$. The curve through the data is a fit to $[(T-T_c)/T_c]^{1/2}$. The plots demonstrate that p scales as $[(T-T_c)/T_c]^{1/2}$ as predicted by Eqs. (7) and (10).

MCT equations even when they are not limited to the first order terms, but rather, Eqs. (5) and (6) are used.[23–25]

When the intermediate power law term is taken into account, the fits result in larger values of the von Schweidler exponent b. Inclusion of the intermediate power law explains the differences between the values of b obtained here and those obtained previously from the salol and OTP susceptibility spectra in the frequency domain[6] and OHD-OKE experiments in the time domain.[3,27] Although the intermediate power law term is not needed to obtain a good fit of the OHD-OKE signal at high T with standard MCT, it is needed even at high temperatures in order to keep the von Schweidler exponent b constant at all temperatures down to T_c.

The intermediate power law region is not consistent with the standard presentations of MCT (A_2 singularity). The exponent parameter c that describes the deviation of the intermediate power law term from the pure logarithmic behavior of the correlation function $f(t)$, is small for all five liquids investigated (see Table I). In salol, $c=0$, which corresponds to the $\log t$ term in $f(t)$ and in the other four liquids, c ranges between 0.1 and 0.2. In this case, the respective term in $f(t)$ is not exactly $\log t$, but instead it is a power law with a small exponent c, $f(t)\propto t^c$. t^c is barely distinguishable from $\log t$, particularly over a limited time range.

As has been shown previously,[39] in time domain data the interval over which the asymptotic power law predictions of MCT can be clearly observed is broader than in frequency domain data. This may explain why in susceptibility spectra the near constant loss contribution is not as readily observed near T_c as is the intermediate power law in OHD-OKE decays. Near constant loss spectra, which resemble logarithmic decays of the correlation function, were seen recently in conductivity spectra of ionic glasses,[40] in dielectric spectra of low molecular weight molecular glasses,[41,42] and in the light scattering spectra of polyisobutylene, poly(methyl methacrylate), and glycerol glasses in the gigahertz frequency range.[43,44] The reason for the NCL spectrum in glasses is not clear, although it is believed that it is unique feature of glasses. Our analysis shows that something akin to the NCL spectrum of glasses exists in the supercooled liquid state at and above T_c.

The observation of the $\sim\log t$ region in the decay of the correlation function in the five molecular liquids studied suggests that a log decay may be a universal feature, at least in molecular liquids. However, the current MCT endpoint or higher order singularity case[13,30,31] does not seem capable of explaining the universality of a $\log t$ term in $f(t)$. Quite the contrary, it is believed that the endpoint case should occur only in very rare situations for systems like colloids that have very specific interparticle interaction potentials. The rarity of the endpoint case comes about because the trajectory of the system in the parameter space of the mode coupling functional normally intersects the boundary of the glass transition hypersurface (endpoint of the glass transition line in the schematic 2 parameter model[31]) with a probability close to zero.

While explanations for $\sim\log t$ decay of the correlation much may be found outside of the context of the MCT, to explain the apparent universality of the $\log t$ portion of the correlation function in terms of the MCT endpoint scheme, we note that in molecular systems, contrary to the schematic models, the phase space of the mode coupling parameters is essentially infinite dimensional because the intermolecular potentials are very complicated. In such a space, one would expect the glass transition hypersurface to have a complex form and complicated, nearly chaotic, boundaries. Therefore, it may be reasonable to assume that any actual trajectory of the system in this space will come into the vicinity of a boundary. It is not necessary for the system to cross the boundary for deviations from the standard two-step relaxation dynamics to occur. If the system is in the vicinity of a higher order singularity, the relaxation behavior will be changed. The proximity of a system to a higher order singularity may explain the differences in the values of the intermediate power law exponents found for the five supercooled liquids. The closer a system's trajectory approaches a higher order singularity, the smaller the exponent c will be in Eq. (11).

It is interesting to note that temperature independent intermediate power laws are also observed in OHD-OKE data from the isotropic phase of liquid crystals near the nematic-isotropic phase transition temperature.[45–47] The intermediate power law exponents are smaller in liquid crystal samples (c is larger) than in the supercooled liquids, and the exponents depend on the aspect ratios of the nematogens.[45–47] If the liquid crystal power law exponent is extrapolated to an aspect ratio of 2.5, the aspect ratio below which a nematic phase no longer exists, the exponent is within the range observed for supercooled liquids. It is possible that the differences in the power law exponents observed in supercooled liquids are a result of structural differences in the molecules. A detailed comparison of dynamics in supercooled liquids and liquid crystals will be presented.[48]

V. CONCLUDING REMARKS

Analysis of the OHD-OKE experiments on BZP, BPM, salol, OTP, and DBP at $T\cong T_c$ and above demonstrates that there is a logarithmic decay or power law decay with a small

exponent ($c<0.2$) of the orientational correlation function in these supercooled liquids. The OHD-OKE experiments measure the time derivative of the polarizability–polarizability correlation function (orientational correlation function). In the OHD-OKE data, the logarithmic or near logarithmic decay of the correlation function appears as the ''intermediate'' power law with exponent ~ -1. The intermediate power law can be observed over a time interval spanning 3–4 decades at $T \sim T_c$ (see Fig. 5). The intermediate power law observed in the five liquids is not consistent with the standard form of mode coupling theory although other features of the data are in agreement with MCT predictions.

A logarithmic decay of the correlation function can be obtained from the endpoint case (A_n, $n \geqslant 3$ singularity) of the MCT. One possible explanation for the intermediate power law is that the MCT higher order singularities are a common feature of relaxation in low molecular weight glass forming liquids rather than being an improbable occurrence. The MCT endpoint case predicts that the OHD-OKE decay will be a power law with exponent -1 or close to -1. It also predicts that the amplitude of the intermediate power law will scale with temperature as $[(T-T_c)/T_c]^{1/2}$. Both the power law with exponent ~ -1 and the temperature scaling are observed experimentally (see Figs. 5–7). As it stands now, the MCT endpoint case needs to be investigated and generalized possibly in the manner discussed qualitatively above. At this time, it is not clear that MCT can account for the observations and other directions of may be required. Gaining an understanding of the intermediate power law may be a key that will unlock a comprehensive description of supercooled liquids and the glass transition.

ACKNOWLEDGMENTS

The authors are grateful to H. C. Anderson, M. Fuchs, W. Götze, K. Ngai, and E. Rössler for helpful discussions. We also thank Dr. N. A. Davydova, for measuring the glass transition temperature of BPM. This research was supported by the National Science Foundation (DMR-0088942).

[1] C. A. Angell, Science **267**, 1924 (1995).
[2] S. D. Gottke, G. Hinze, D. D. Brace, and M. D. Fayer, J. Phys. Chem. **105**, 238 (2001).
[3] G. Hinze, D. D. Brace, S. D. Gottke, and M. D. Fayer, J. Chem. Phys. **113**, 3723 (2000).
[4] D. D. Brace, S. D. Gottke, H. Cang, and M. D. Fayer, J. Chem. Phys. **116**, 1598 (2002).
[5] W. Götze, *Liquids, Freezing, and Glass Transition* (Elsevier, New York, 1989).
[6] W. Götze and L. Sjögren, Rep. Prog. Phys. **55**, 241 (1992).
[7] S. Kämmerer, W. Kob, and R. Schilling, Phys. Rev. E **56**, 5450 (1997).
[8] S. Kämmerer, W. Kob, and R. Schilling, Phys. Rev. E **58**, 2141 (1998).
[9] R. Schilling and T. Scheidsteger, Phys. Rev. E **56**, 2932 (1997).
[10] W. Götze, J. Phys.: Condens. Matter **11**, A1 (1999).
[11] L. Fabbian, W. Götze, F. Sciortino, P. Tartaglia, and F. Thiery, Phys. Rev. E **60**, 2430 (1999).
[12] L. Fabbian, W. Götze, F. Sciortino, P. Tartaglia, and F. Thiery, Phys. Rev. E **59**, R1347 (1999).
[13] J. Bergenholtz and M. Fuchs, Phys. Rev. E **59**, 5706 (1999).
[14] K. Dawson, G. Fo, M. Fuchs, W. Götze, F. Sciortino, M. Sperl, P. Tartaglia, T. Voigtmann, and E. Zaccarelli, Phys. Rev. E **63**, 011401 (2001).
[15] A. M. Puertas, M. Fuchs, and M. E. Cates, Phys. Rev. Lett. **88**, 098301 (2002).
[16] F. Mallamace, P. Gambadauro, N. Micali, P. Tartaglia, C. Liao, and S.-H. Chen, Phys. Rev. Lett. **84**, 5431 (2000).
[17] D. McMorrow, W. T. Lotshaw, and G. Kenney-Wallace, IEEE J. Quantum Electron. **24**, 443 (1988).
[18] D. McMorrow and W. T. Lotshaw, J. Phys. Chem. **95**, 10395 (1991).
[19] S. Ruhman, L. R. Williams, A. G. Joly, B. Kohler, and K. A. Nelson, J. Phys. Chem. **91**, 2237 (1987).
[20] F. W. Deeg and M. D. Fayer, J. Chem. Phys. **91**, 2269 (1989).
[21] S. Kinoshita, Y. Kai, M. Yamaguchi, and T. Yagi, Phys. Rev. Lett. **75**, 148 (1995).
[22] Y. Kai, S. Kinoshita, M. Yamaguchi, and T. Yagi, J. Mol. Liq. **65–66**, 413 (1995).
[23] E. Bartsch, Transp. Theory Stat. Phys. **24**, 1125 (1995).
[24] W. Götze, J. Phys.: Condens. Matter **2**, 8485 (1990).
[25] G. Li, G. M. Fuchs, W. M. Du, A. Latz, N. J. Tao, J. Hernandez, W. Götze, and H. Z. Cummins, J. Non-Cryst. Solids **172**, 43 (1994).
[26] A. Tölle, H. Schober, J. Wuttke, and F. Fujara, Phys. Rev. E **56**, 809 (1997).
[27] G. Hinze, D. D. Brace, S. D. Gottke, and M. D. Fayer, Phys. Rev. Lett. **84**, 2437 (2000).
[28] J. Wuttke, M. Kiebel, E. Bartsch, F. Fujara, W. Petry, and H. Sillescu, Z. Phys. B: Condens. Matter **91**, 357 (1993).
[29] E. Bartsch, V. Frenz, J. Baschnagel, W. Schaertl, and H. Sillescu, J. Chem. Phys. **106**, 3743 (1997).
[30] W. Gotze and M. Sperl, Phys. Rev. E **66**, 011405 (2002).
[31] W. Götze and R. Haussmann, Z. Phys. B: Condens. Matter **72**, 403 (1988).
[32] N. A. Smith and S. R. Meech, Int. Rev. Phys. Chem. **21**, 75 (2002).
[33] P. P. Ho and R. R. Alfano, Phys. Rev. A **20**, 2170 (1979).
[34] W. T. Lotshaw, D. McMorrow, C. Kalpouzos, and G. A. Kenney-Wallace, Chem. Phys. Lett. **136**, 323 (1987).
[35] H. Cang, V. N. Novikov, and M. D. Fayer, Phys. Rev. Lett. (submitted).
[36] N. A. Davydova (private communication, 2001).
[37] N. A. Davydova, V. I. Mel'nik, K. I. Neipovitch *et al.*, J. Mol. Struct. **563–564**, 105 (2001).
[38] C. J. F. Böttcher and P. Bordewijk, *Theory of Electric Polarization* (Elsevier, Amsterdam, 1992).
[39] T. Franosch, M. Fuchs, W. Goetze, M. R. Mayr, and A. P. Singh, Phys. Rev. E **55**, 7153 (1997).
[40] K. L. Ngai, J. Phys. Chem. **110**, 10576 (1999).
[41] P. Lunkenheimer, U. Schneider, R. Brand, and A. Loidl, Contemp. Phys. **41**, 15 (2000).
[42] A. Kudlik, S. Benkhof, R. Lenk, and E. Rössler, J. Mol. Struct. **479**, 201 (1999).
[43] A. P. Sokolov, A. Kisliuk, V. N. Novikov *et al.*, Phys. Rev. B **63**, 172204 (2001).
[44] A. Kisliuk, V. N. Novikov, and A. P. Sokolov, J. Polym. Sci., Part B: Polym. Phys. **40**, 201 (2002).
[45] S. D. Gottke, D. D. Brace, H. Cang, and M. D. Fayer, J. Chem. Phys. **116**, 360 (2002).
[46] S. D. Gottke, H. Cang, B. Bagchi, and M. D. Fayer, J. Chem. Phys. **116**, 6339 (2002).
[47] H. Cang, J. Li, and M. D. Fayer, Chem. Phys. Lett. **366**, 82 (2002).
[48] H. Cang, J. Li, V. N. Novikov, and M. D. Fayer, J. Chem. Phys. (to be published).